The Radiative Shock Clump Regime: When Do Heterogenous Flows Cool?

ABSTRACT

In simulations of the canonical *shocked-clump* model, when radiative cooling is included it may be unclear for which of the shocks in the system the cooling is important. Understanding this is critical, as cooling can have a large effect on the evolution of a heterogeneous system; in particular, radiative cooling can lead otherwise diffuse material to become self-gravitating. We here present a way to determine, based on the densities and Mach numbers of the flow, when radiative cooling may be important. The results are derived from consideration of the *cooling timescale* of 1) the shock transmitted into the clump and 2) the clump bow shock. We include synthetic Schlieren images indicative of the different parameter regimes and discuss their differing morphologies and observational implications.

Subject headings:

1. Introduction

AF OK I will edit this

Radiative cooling is an important contributor in astrophysical behavior. Just by virtue of the fact that we can see them, we know that many objects are radiating appreciable amounts of their energy away. This must have a dramatic effect on their morphology. The loss of energy has a huge impact on the ability of cloud-cores to collapse in the event of some trigger mechanism like a super-nova blast. Numerical modeling shows that without removing some of the energy added by the shock, these clouds would most likely re-expand to cool adiabatically, not collapse beyond the point of the Jean's Mass.

Because of the extreme range of conditions in molecular clouds, computer simulations are used to model their large-scale behavior. The majority of these simulations have been done using either an adiabatic equation of state (EOS) or very near an isothermal EOS to mimic the effects of cooling. Now we are reaching a point where accurate modeling of cooling tracks is very feasible and necessary to capture a real glimpse of the physics predicating these structures. Here, we derive and explore a parameter space to determine whether or not including the effects of cooling will have an influence on the evolution of the system.

This analysis is sensitive to the specifics of the method that we use to handle radiative cooling. Many codes have tried to implement accurate cooling routines, but accurately simulating the post-shock conditions in these flows is very difficult because of the complexity of the environment. Typical cooling routines include a look-up table that lists the expected cooling rate from a gas of a certain temperature and bases that estimation on ionization equilibrium conditions in the post-shock flow. This approach is insufficient, as post-shock gas can be far from ionization equilibrium. This situation drastically changes the amount of energy expected to be emitted from a shocked gas.

[1]Los Alamos National Laboratory, Los Alamos, NM 87544

[2]Department of Physics and Astronomy, University of Rochester, Rochester, NY 14620

We present a series of analysis describing the conditions where radiative cooling plays a strong role in the behavior of shock-cloud interactions for different methods of accounting for radiative cooling. Section 2 describes a first approximation using an analytic cooling curve. Section 3 describes more detailed methods of cooling, and the results of simulations carried out with a varying degree of realism for post-shock behavior. Finally, Section 4 presents evidence of the extreme effects that radiative cooling can have on the overall morphology, mixing, and dynamics of a supersonic wind interacting in a highly inhomogeneous medium.

[[[KY: My old bullet points follow.

- ambiguity with respect to location of cooling in simulations, and the strength of the cooling (in some cases).
- The role of cooling is described by the ratio of the cooling timescale and the dynamical timescale.
- People appreciate that if the cooling timescale is comparable or less than the dynamical timescale, then it will be important. The novelty of this work is that we recognize that there are multiple shocks in the shocked-clump system, and therefore they may have differing cooling properties.
- When cooling isn't present, morphology is [...poofy, smooth...]
- When cooling is present, morphology is [...enhanced KH/RT, fragmentation...]
- Somewhere should note pat's 1989 paper, discuss how this is similar but not just a repeat.
-

]]]

2. Physics and model

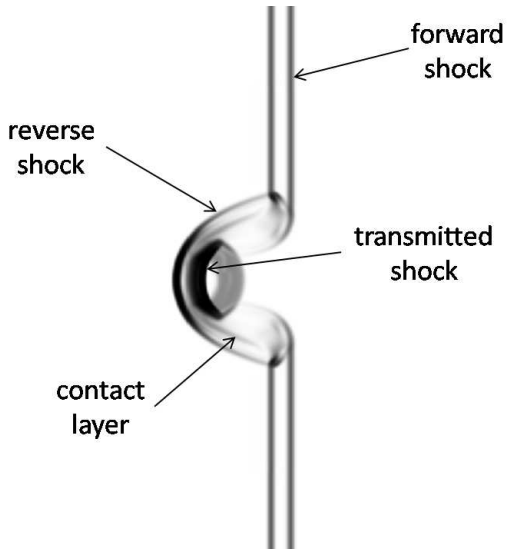

Fig. 1.— Diagram illustrating the nomenclature of the shocked-clump system. From [afrank2011].

In the simple shocked-clump model, a planar shock sweeps over a dense sphere. There are three main shocks: the *incident shock*, the shock transmitted into the clump as the incident shock sweeps over it (*transmitted shock*), and the bow shock which forms and propagates reverse of the incident shock (*bow shock*). There are therefore three different locations where radiative cooling may be playing a role, and as such separate treatment of all three is important. Here, we will exclude analysis of the incident shock, since its primary role is as instigator of the evolution of the other two, and therefore its cooling quickly (i.e. $t < t_{cc}$) becomes comparatively unimportant.

We begin with the consideration that a given material has a cooling timescale associated with it [cite],

$$t_{cool} = -\frac{3k_B}{2n} \int_T^{T/2} \frac{dT}{\Lambda(T)} \tag{1}$$

where k_B is Boltzmann's constant, n the number density, T temperature, and $\Lambda(T)$ the cooling function. In a shocked-clump system, the typical dynamical timescale is the *cloud-crushing timescale* of cite[kmc1994],

$$t_{cc} = \frac{\sqrt{\chi} r_c}{M c_s} \tag{2}$$

where χ is the clump to surrounding background (*ambient*) density ratio, r_c the radius of the clump, c_s the sound speed in the preshock ambient medium and M the Mach number of the incident shock; see Figure 1.

Cooling will therefore be important if $t_{cool} \lesssim t_{cc}$—if $t_{cool} \gg t_{cc}$, the system will evolve hydrodynamically before it has a chance to cool significantly. One main impact of cooling is that the removal of thermal energy behind a shock can reduce the shock's propagation speed [citewho?]. Note that if $t_{cool} \ll t_{cc}$, the system essentially behaves isothermally [cite]. (One may analogously describe the cooling in terms of length scales, in which case if the cooling length scale is comparable to or less than the clump radius then cooling will be

important.) As discussed in the introduction, there exist systems which are stable (i.e., not actively diffusing or clumping) compared to a typical shock-crossing time for that system. Hence, it may be possible to have a system of a shock running over a clump which results in radiative cooling being activated in the post-shock material. Therefore, a correct discussion of the dynamics of that system requires an understanding of which of the various shocks may be radiative.

We can define the cooling time as the time it takes for a parcel to cool to half its initial temperature as in Eq. 1. For a just-shocked parcel, the initial temperature will be the post-shock temperature given by the Rankine-Hugoniot jump conditions in the high Mach number limit,

$$T_{ps} = \frac{3X_\mu}{16k_B} v_s^2 \tag{3}$$

This expression is correct for the initial shock in the system, $T_{ps,i}$.

In order to use the above further, we need expressions for the postshock temperature for the bow and transmitted shocks. The transmitted shock is easier, just involving a factor of χ [cite],

$$T_{ps,t} = \frac{3X_\mu}{16k_B} \frac{v_s^2}{\chi} \tag{4}$$

For the bow shock, we can make a close approximation of simply

$$T_{ps,b} = \frac{3X_\mu}{16k_B} v_s^2 = T_{ps,i} \tag{5}$$

In practice, the bow shock temperature will be slightly lower than this, partially due to the multidimensional nature of the problem and the consideration that the bow shock is a relatively weak shock, so assumptions in Eq. 3 may not be appropriate. For the present study, we believe the details of this discrepancy to be of minor importance.

The task now is to specify the cooling function in Eq. 1, and investigate four cases: 1) neither transmitted nor bow shock are cooling, 2) only transmitted is cooling, 3) only bow is cooling, or 4) both are cooling. We proceed by considering two different forms of the cooling function.

2.1. Power law cooling

It is typical to describe the cooling function as a simple power law [cites]. In fact, such treatment is only appropriate above $T = 1e8$ K, where Bremsstrahlung dominates. Nonetheless, adopting a power law form can be instructive on the effects of cooling and therefore worthwhile.

The cooling function $\Lambda(T)$ in power law form in general is

$$\Lambda(T) = \alpha T^\beta \tag{6}$$

where α and β are free parameters (note that for Bremsstrahlung, $\beta = 1/2$ [cite]). Using Eq. 6, the condition $t_{cool} \lesssim t_{cc}$ becomes

$$-\frac{3k_B}{2n} \int_T^{T/2} \alpha^{-1} T^{-\beta} dT \lesssim \frac{\sqrt{\chi} r_c}{M c_s} \tag{7}$$

$$\Rightarrow \frac{3k_B}{2n\alpha} \frac{(2^{\beta-1} - 1)T^{1-\beta}}{\beta - 1} \lesssim \frac{\sqrt{\chi} r_c}{M c_s} \tag{8}$$

We may represent this result via a plot of two-dimensional parameter space in logarithmic density contrast χ and velocity of the incident shock v. [[[The remaining variable, the post-shock temperature T, is given as a function of M and χ in Eq. 3–5 for the different shocks.]]]

Figure 2 plots the parameter space for analytic-form cooling. The result maps out several regions in the parameter space: blue areas have neither shock cooling, red transmitted shock only, green bow shock only, and finally yellow has both shocks cooling. As can be seen, as the product of clump density and clump radius increases, cooling is triggered both over a broader parameter space, and for an increasing number of shocks. Indeed, at the highest density & radius (lower-right panel), most of the paramter space falls under the "both shocks cooling" regime. Note also that this analysis implies that below a certain density & size limit, it is impossible to have the bow shock cooling at all. [[[KY: possibly because only possible if nclump<namb or something? white spaces?]]] Finally, it is clear that under power-law cooling, transmitted-shock-only cooling favors high shock speeds and large density contrasts χ, whereas bow-shock-only cooling favors low shock speeds and lower density contrasts.

2.2. More realistic cooling

Cite[Raymond1976] provides a detailed 1D cooling shock modeling code which incorporates *non-equilibrium cooling*, i.e. hydrogen ionization-recombination, hydrogen excitation, and metal excitation. One way in particular that this may deviate from power law cooling is that the effects of metal excitation become very important below roughly 20,000K, where hydrogen begins to recombine. Details on the implementation may be found in the above citation.

If we implicitly use this code for the cooling function in Eq. 1, then we may generate a parameter space diagram analogous to Fig. 2. This is offered in Fig. 3. The resulting plot shows similarities, although there are important differences as well. The most striking of which is that the region which supports bow shock cooling is nearly perpendicular in this parameter space to that which supports transmitted shock cooling. This is in contrast to power law cooling, where there were obvious correlations between χ and v_s to either bow-shock-only or transmitted-shock-only. Instead, regions which allow neither shock to cool can be found over a wide range of this paramter space. Moreover, whereas in the previous panel where $nr_c = 10^4$ (upper left), no bow shock cooling was capable, here we see a substantial range of parameters which supports it.

We present these more sophisticated results to illustrate one way in which a power law assumption may not be fully accurate. Nonetheless, the physics associated with the corresponding regions should be consistent. That is, that simulations of material in a "blue" region of Fig. 2 should appear analogous to material in a "blue" region of Fig. 3. Therefore, in the next section we offer the results from hydrodynamic simulation.

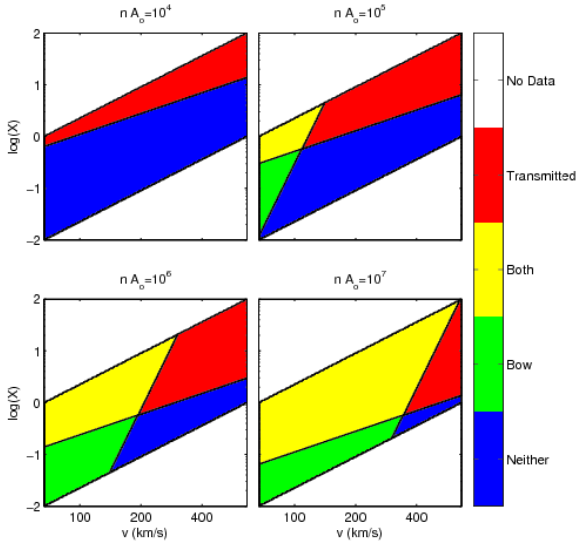

Fig. 2.— Depiction of parameter space for a power-law cooling function, $\Lambda(T) \propto T^{\beta}$. blue areas have neither shock cooling, red transmitted shock only, green bow shock only, and finally yellow has both shocks cooling. [[[The points labelled A–D indicate the locations of the simulations shown in Fig. 4 as discussed below. —But we're still doing DM? ∼KY]]]

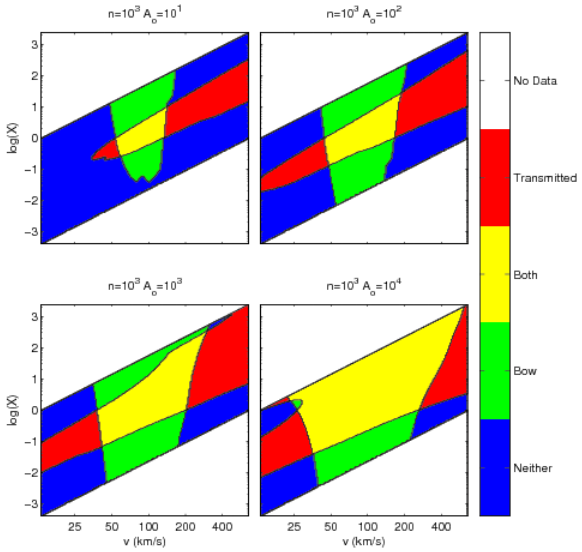

Fig. 3.— Depiction of parameter space for a more sophisticated cooling function. As before, blue areas have neither shock cooling, red transmitted shock only, green bow shock only, and finally yellow both shocks cooling.

3. Results

Parameter	Value
n_{amb}	250 cm^{-3}
T_{amb}	100 K
r_c	100 AU
χ	10

Table 1: Table showing parameters common to all cases given in Table 2.

Run	Case	v_{wind} [km/s]	t_{cc} [yr]	T_{bow} [10^5 K]	T_{trans} [10^4 K]	L_{bow} [r_c]	$L_{trans}[r_c]$	Cooling src?
A	Neither	200	0.75	9.02	9.02	39.3	1.41	F
B	Transmitted	200	0.75	9.02	9.02	39.3	1.41	T
C	Bow	50	3.00	0.564	0.564	0.273	7.86	T
D	Both	400	0.375	36.1	36.1	1.88×10^3	0.211	T

Table 2: Table of runs depicted in Fig. 4. The Run name corresponds to the Row name in that Figure. The last column indicates whether the cooling source term was turned on.

To illustrate the morphological impacts of the different cooling scenarios, we carried out simulations in each region of the parameter space. The various fundamental and derived parameters are given in Tables 1 and 2. The simulations were carried out in cylindrical symmetry. We use a hyperbolic tangent profile to "smooth" the transition from the center of the clump (*clump core*, [shu2008]) to the ambient background of extent XXX%. An initially planar shock is set up and sweeps over the clump. Time $t = 0$ is taken to be the time when the shock first meets the edge of the clump; subsequent times are given in units of cloud-crushing time t_{cc} from Eq. 2. As the impact is independent of the particulars of what cooling scheme is used, for simplicity we adopt power-law cooling with parameters from Eq. 6 of $\alpha = ...$ and $\beta = ...$, respectively. The locations in the parameter space are given as points A–D in Fig. 2.

Figure 4 provides examples of the four different regimes of shock cooling in the shocked-clump model. Each case is depicted at three different times: 0.6957, 1.4546, and 2.2136 t_{cc}. When neither shock is cooling (row A), the bow shock moves upstream until it loses the pressure support from the ablated, upswept clump at $t > t_{cc}$. In this case, the speed of the transmitted shock is well-described by $v_{ts} = v_s/\chi$ which is derived from simple ram pressure balance considerations. Note finally that in all cases, owing to the presence of cooling the initially planar single shock separates into two (or more). [[[KY: row A is w/o cooling source term, right?]]]

When the transmitted shock only is cooling, row B, the bow shock grows and achieves a bow-shock stand-off distance of $\sim 0.5r_c$, much as before. However, the speed of the transmitted shock is reduced, implying that the simple relation between v_{ts} and v_s given above will be incorrect: indeed, comparison of the first panel in rows A and B show a markedly reduced v_{ts} in row B. As discussed in cite[yirak2010], this can present difficulties in correctly simulating such a system, as it drives a strong constraint on the necessary resolution to maintain an adequately-resolved cooling length. The decreased distance between the transmitted shock and the bow shock/transmitted shock contact layer—as well as the continual crushing of the rest of the surface of the clump—also produces shorter Kelvin-Helmholtz (KH) and Rayleigh-Taylor (RT) growth rates cite[fragile2008, yirak2010]. This in turn produces increased fragmentation of the clump during the ablation process, potentially leading to the creation of self-gravitating clumps [cite who? falle?]. Finally,

we note that, while the reduced v_{ts} might lead to an expected increase in t_{cc}, in fact the fragmentation leads to a clump which is driven to smaller scales and processed much more rapidly.

When the bow shock only is cooling, row C, the bow shock standoff distance is reduced. In the extreme case of strong cooling, the bow shock may wrap tightly around the ablation surface cite[mellema2002, fragile2004, yirak2009, yirak2010]. Again, in the case of strong cooling, this can now both enhance instability growth and place a constraint on desired resolution. With extreme cooling, citep[yirak2010], the bow shock may collapse onto the contact, resulting in much enhanced fragmentation of the ablation front/contact layer. In the case presented here, bow-shock-only cooling resembles neither-cooling much moreso than transmitted-shock-only. There remains clear separation between the bow, contact, and transmitted shock; the transmitted shock is near-planar; the main location of vorticity generation appears to be near $r = r_c$. It is interesting to note that the location of the [quadruple point?], caused by the bow shock reflection interacting with the initial shock separation, has a reduced radial velocity component in this case. This could be of importance because of the possible role such shock-shock interaction regions have on emission in e.g. Herbig-Haro objects cite[Pat, mach stems].

Finally, in panel D, when both shocks are cooling the result is essentially a superposition of the preceding two scenarios. This presents potentially the largest chance for errors from a numerical standpoint. From a morphological standpoint, the bow shock/ablation region (contact)/transmitted shock reduce to a very small fraction of the clump radius r_c, in turn greatly enhancing KH/RT growth and resulting in a scenario where most of the clump material is stripped off-axis and embedded in a highly-dynamic "froth". This case bears the closest resemblence to the transmitted-shock-only case of row B for that material which does not yet have a large axial velocity component—that is, material near-axis is compact in the z-direction with large vortical motions. This is in contrast to rows A and C (neither-cooling, bow-only cooling), for which the axial material exhibits distinct multiple shocks.

3.1. Emission implications

As discussed above, the two main impacts of cooling on the shocked-clump system are to 1) reduce the spatial scale of the various features, and 2) decrease instability growth times, thereby enhancing vorticity generation.

[[[KY: If we aren't going to have synthetic emission images (?), then any discussion of emission should probably be shunted to the discussion section.]]]

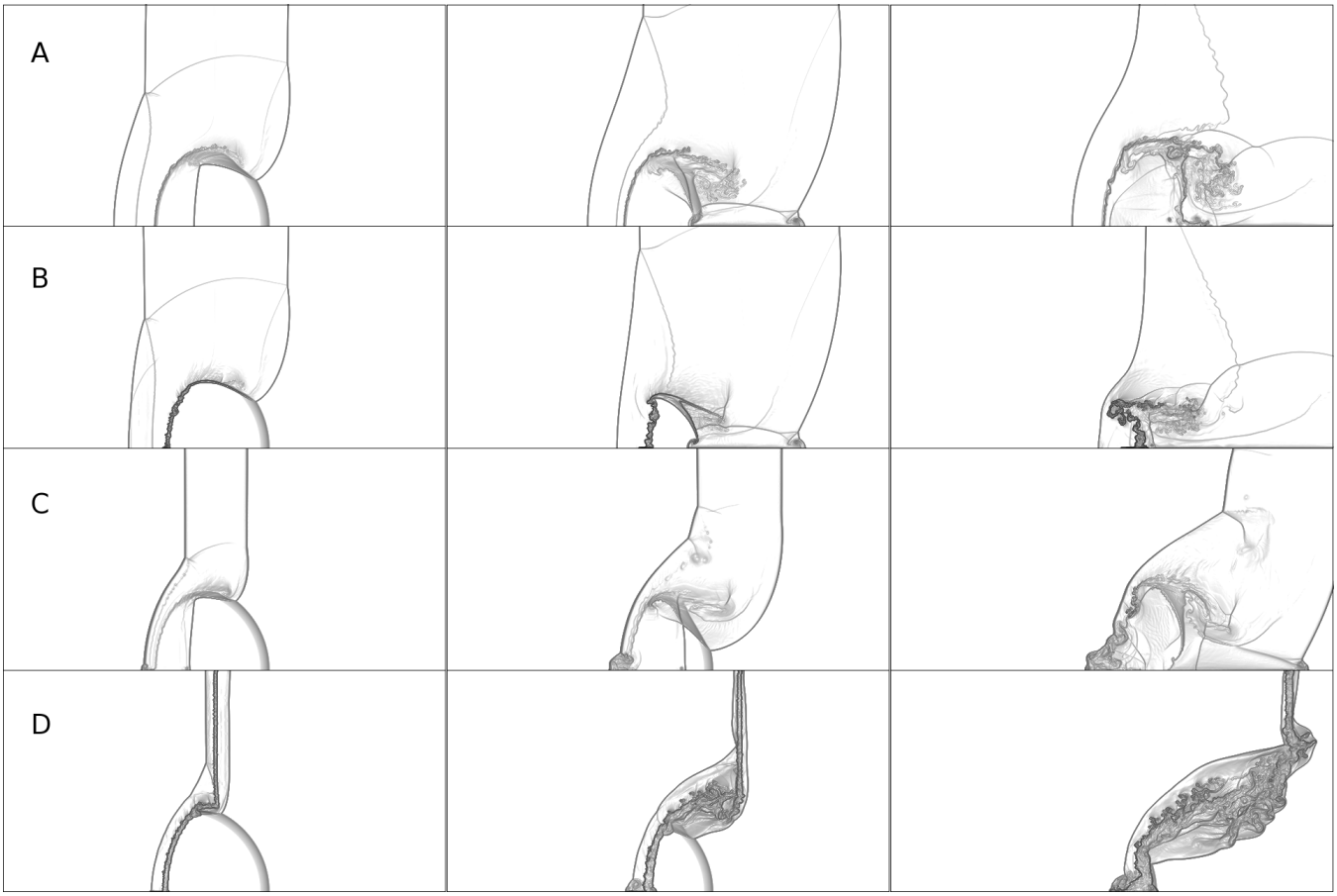

Fig. 4.— Four simulation results meant to be indicative of the four different scenarios, each at three different times, as discussed in Section 3. Rows A–D correspond to neither shock cooling, transmitted shock only, bow shock only, or both shocks cooling, respectively.

4. Discussion and conclusion

- Morphological impact? Synthetic emission results...
- mention 3d (vishniac...), heat conduction (orlando), B fields (Shu & Stone), kappa-epsilon maybe?
- Impact of paper is that it clarifies longstanding ambiguity & should help those that wish to study a particular regime (or converse for observers). Updates 1989 because cooling is related to emission (the focus of that work). Provides another tool to help analyze more complex flows like hosts of clumps (cite MHD clumps paper).